Journal of Alloys and Compounds 489 (2010) 343–347

Contents lists available at ScienceDirect

Journal of Alloys and Compounds

journal homepage: www.elsevier.com/locate/jallcom

A simple route to synthesize CuS framework with porosity

Minmin Li [a], Qingsheng Wu [a,*], Jianlin Shi [b]

[a] Department of Chemistry, Tongji University, 1239 Siping Road, Shanghai 200092, PR China
[b] Shanghai Institute of Ceramics, Chinese Academy of Sciences, 1295 Dingxi Road, Shanghai 200050, PR China

ARTICLE INFO

Article history:
Received 30 June 2009
Received in revised form
17 September 2009
Accepted 22 September 2009
Available online 30 September 2009

Keywords:
CuS
Porous structure
Chitosan

ABSTRACT

A simple route was developed to one-step synthesis of CuS framework with porosity via hydrothermal method using chitosan as template. The BET surface area of as-obtained CuS sample was measured to be 31.72 m^2/g and the single point adsorption total pore volume was measured to be 0.1367 cm^3/g. The effect of various experimental conditions, including temperature and reagents for the growth of CuS porous structure was investigated. Increase of reaction temperature led to the transformation of morphologies from porous structure to three-dimensional superstructure. The change of copper salt also resulted in great change of the morphologies of CuS samples. The UV–vis absorption and XRD patterns of the CuS samples with different morphologies changed accordingly. Based on the evidence of electron microscope images, the formation mechanism of porous-structured CuS has been proposed. The presence of chitosan in this process is crucial because of their repulsion of charged groups and a coordination effect with Cu^{2+}.

1. Introduction

To date, semiconductors with different morphologies are promising for quantum confinement effect studies and important candidates for potential sensor, solar cell applications and nanometer-scale switches [1–7]. In this field, the assembly of nano-scale building blocks into hierarchical and complex nanostructures and porous structures has become the focus of many studies because it offers opportunities in the search for exciting new properties of semiconductor materials and helps to fabricate functional micro- and nano-devices, catalysts, drug-carriers, etc. [8–11]. In recent years many efforts have been focused on the assembly of lower dimensional nanostructures into three-dimensional ordered superstructures, such as multipods, snowflakes, dendritic structures [12–14].

Copper sulfide has attracted attention of many materials workers because of its unique properties and wide application in many fields, such as in thermoelectric cooling material, optical recording material, optical filter, solar cell, superionic materials, and the materials in chemical sensors [15–20]. Various kinds of structures of CuS have been synthesized recently. For example CuS superstructures have been reported by Zhou's and Xie's research group, respectively [22,21]. And the synthesis of porous CuS was scarcely reported, such as copper sulfide hollow spheres by self-assembly coupled with H_2S bubble templating [23] and CuS hollow spheres by the TGA-assisted hydrothermal method [24]. In our paper CuS porous nanostructure (not hollow spheres) assembled by nanoparticles in the assistance of chitosan was reported and the transformation from porous structure to three-dimensional nanostructure based on the simple change of experimental conditions was attained. In this article, taking the preparation of CuS nanostructures as an example, the mechanism of cupric-chitosan system is elucidated on the basis of electronic images and parallel experiments.

2. Experimental

2.1. Preparation of two kinds of CuS nanostructures

Chitosan was purchased from Golden-Shell Biochemical Co. (Zhejiang, China). The N-deacetylation was 90%. Copper sulfate ($CuSO_4 \cdot 5H_2O$), copper acetate ($Cu(Ac)_2 \cdot H_2O$), thiourea, and acetic acid were all chemically pure. The water used in experimental process was deionized water.

Typically, 0.015 g chitosan was dissolved in HAc water solution with 1% HAc water solution and stirred for some time to ensure dissolution perfectly. Then 1 mmol $Cu(Ac)_2 \cdot H_2O$ and 3 mmol thiourea were added. The suspension was transferred into a Teflon-lined stainless steel autoclave with 20 mL capacity. The reactions were carried out in a digital-type temperature-controlled oven and the autoclaves were sealed and maintained constantly at 100 °C for 4 h. The autoclaves were cooled to room temperature naturally when the reaction finished. The precipitation was separated by centrifugation and washed with HAc solution and absolute alcohol subsequently. Finally the as-obtained products were dried under vacuum at 60 °C for further characterization. The comparative experiment was performed substituting $CuSO_4 \cdot 5H_2O$ for $Cu(Ac)_2 \cdot H_2O$ to explore the forming mechanism of CuS.

2.2. Characterization

The samples were characterized by many means. The X-ray diffraction (XRD) patterns were recorded using a Bruker AXS, D8 Focus diffractometer with graphite

* Corresponding author. Tel.: +86 21 6598 2620; fax: +86 21 6598 1097.
E-mail address: qswu@tongji.edu.cn (Q. Wu).

0925-8388/$ – see front matter © 2009 Published by Elsevier B.V.
doi:10.1016/j.jallcom.2009.09.129

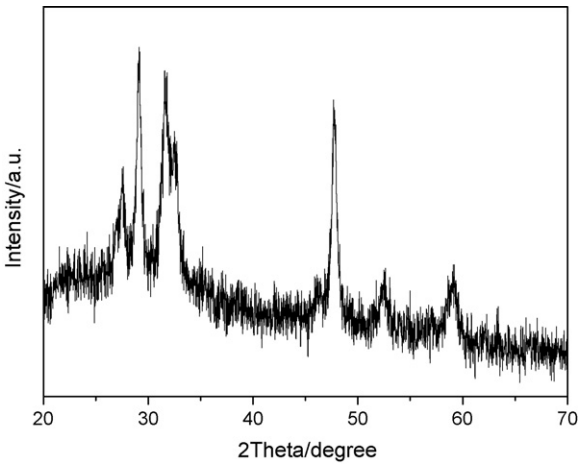

Fig. 1. XRD pattern of prepared CuS sample at 90 °C after hydrothermal process for 4 h.

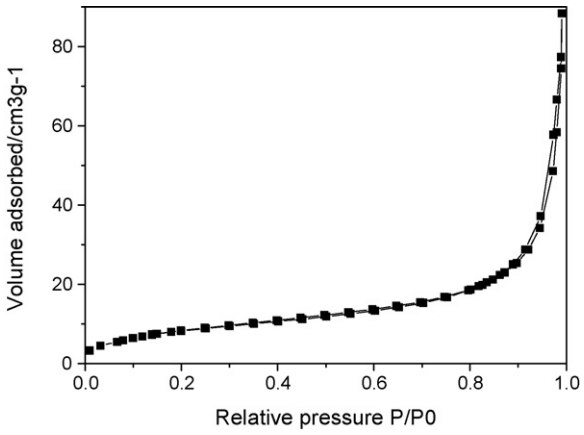

Fig. 3. Nitrogen adsorption/desorption isotherms of CuS sample.

monochromatized Cu KR irradiation (λ = 1.5418 Å). Scanning electron microscopy (SEM) images were measured on a Philips XL-30E scanning electron microscope by dropping products' suspension on a glass sheet. Transmission electron microscopy (TEM) images and electron diffraction (ED) were observed on JEOL JEM-2010, at an accelerating voltage of 200 kV. UV–visible absorbance spectra (UV–vis) were recorded on an Agilent 8453 spectrophotometer. The nitrogen absorption and desorption isotherms were recorded using Tristar 3000 system.

3. Results and discussion

Firstly, XRD patterns of samples were investigated and shown in Fig. 1 to ascertain the structure of samples. Hexagonal CuS obtained after hydrothermal treatment for 4 h at 90 °C was exhibited in Fig. 1. All diffraction peaks can be indexed to the hexagonal CuS (JCPDS 06-0464) with lattice constants a = 3.804 Å and c = 16.378 Å. The average particles size of the sample calculated on the basis of Deby–Scherrer formula was around 18.4 nm.

To verify the particles size of the sample and observe the inner morphology of the sample, TEM was used to characterize the morphology and nanostructure of CuS nanomaterials at 90 °C in Fig. 2. We can see from the ordinary TEM image that nanospheres with the diameter of about 100–200 nm were synthesized in the large scale under hydrothermal condition. And the shell of these nanospheres was not smooth and had rug surface, which implied the inner structure of these nanospheres. The amplified TEM image was observed to explore the inner structure further in Fig. 2b. It showed that these nanospheres all mainly included two sections: a relatively solid core and a porous shell. These pores were formed by fine particles of CuS in the assistance of chitosan under hydrothermal condition and they were irregular because they were located in the clearance among the fine CuS particles with random arrangement. The ED revealed the fine particles which self-assembled into nanospheres were polycrystalline. All TEM and ED results corresponded with the XRD results.

For the purpose of illustration of porous structure of CuS further, Brunnauer–Emmett–Teller (BET) gas sorptometry measurements were used to characterize pore volume, pore diameter and specific surface area in Fig. 3. The N_2 adsorption/desorption isotherms of the synthesized CuS sample exhibited typical type-III hysteresis, indicative of the presence of pores. The H_2-hysteresis loops at relative pressure (P/P_0) above 0.8 were present, suggesting the adsorption of N_2 molecules in the intra-particle voids. The BET surface area was measured to be 31.72 m^2/g and the single point adsorption total pore volume was measured to be 0.1367 cm^3/g. The average pore size of 17 nm was calculated with the Barett–Joyner–Halenda (BJH) method.

The influence factors such as temperature and reagent were examined. The SEM and TEM images in Fig. 4 showed the morphologies of synthesized products at different temperatures. Obtained samples all had clear porosity when reaction was performed at lower temperature (90 °C) in Fig. 4a. When the temperature was up to 105 °C, some CuS nanoparticles began to aggregate together to become solid. And the other CuS nanoparticles remained to keep porous structure (Fig. 4b). When the temperature was up to 140 °C, CuS solid nanospheres but porous nanospheres appeared in the large scale in the TEM image (Fig. 4c). To discern the morphology of CuS nanospheres, SEM was used to observe subtly the surface structure (Fig. 4d). From the SEM image, we could see that rectangular CuS thin flakes with width of 50–100 nm and thickness of about 20 nm were self-assembled of nanospheres. What we needed to emphasize was that these spheres were similar in size at different temperatures whichever structures they had. The results indicated that the self-assembly of the nanoparticles was distinctly different in the reaction system under hydrothermal condition at different temperatures and thus the

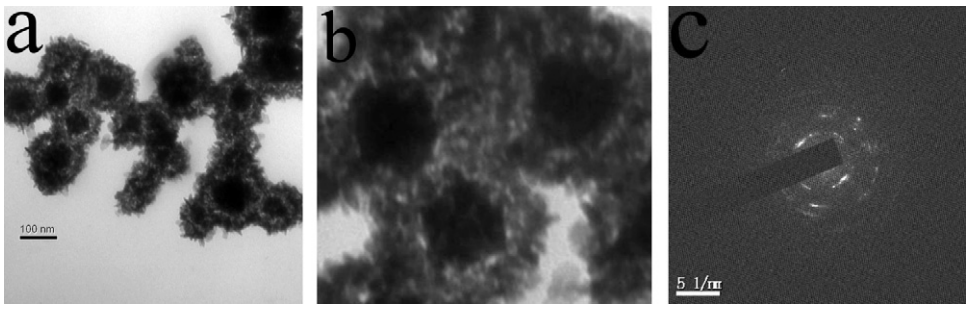

Fig. 2. TEM images of prepared CuS sample at 90 °C after hydrothermal process for 4 h. (a) The ordinary TEM image, (b) the amplified TEM image and (c) ED image.

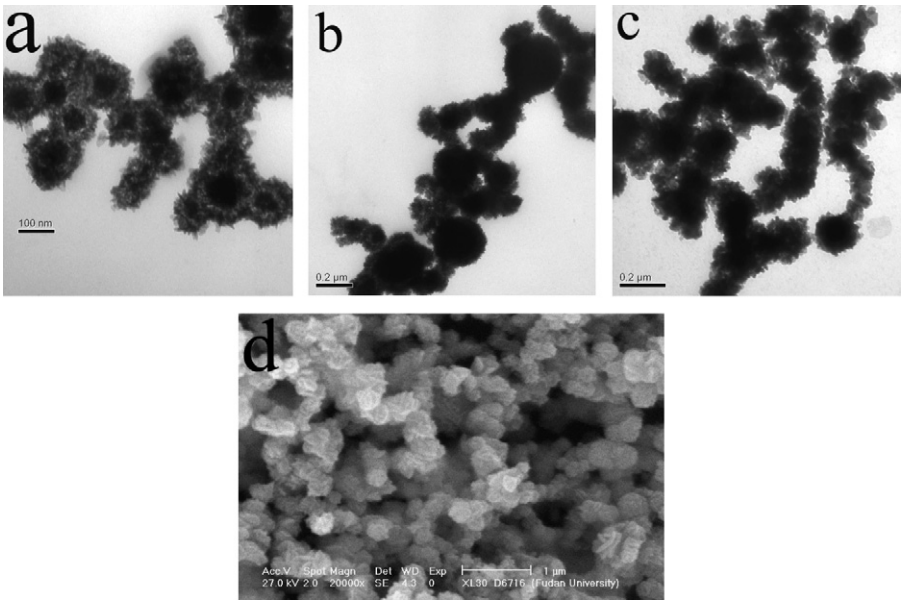

Fig. 4. CuS samples with different morphologies at different temperatures. (a) TEM image at 90 °C, (b) TEM image at 105 °C and (c, d) TEM and SEM images at 140 °C.

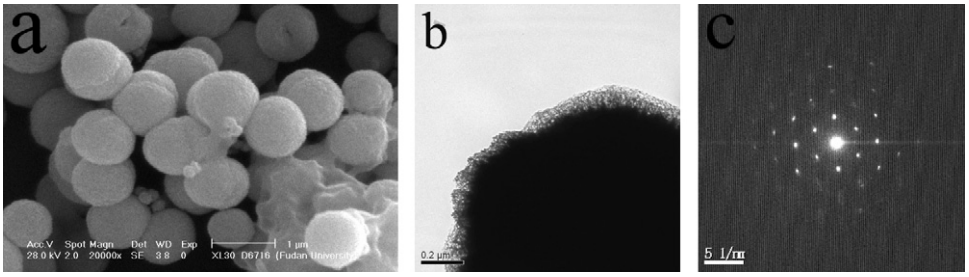

Fig. 5. CuS sample when copper sulfate was used as the source of sulfur and other conditions remained. (a) SEM image, (b) TEM image and (c) ED image.

morphologies of the as-obtained samples depend on the temperature. Lower temperature gave a mild environment, in which the crystal growth was slow and it is possible for the formation of porous structure. With the increase of temperature, the bonds between chitosan and copper ions became weaker, which made chitosan break away from copper ions easier. Hence the function of impeding fine particles collecting resulted from the NH_2^+ groups in the molecule of chitosan enervated gradually. The three-dimensional superstructures with intense self-assemble were formed.

In order to understand the functions of anion in the formation of metal sulfide nanostructures, the phenomena occurring in the present solution with different anions were observed. Copper sulfate substitute for copper acetate was introduced into the reaction system, aggregated CuS microspheres with the diameter of about 1 μm were obtained and these microspheres had a rugged surface (in Fig. 5a). TEM result verified this phenomenon further (Fig. 5b). ED was used to further investigate the CuS crystal status and growth of CuS microspheres. The spatial arrangement of the spots in the ED images revealed the set of lattice planes derived from a single hexagonal crystal.

For the purpose of investigating the reason why the morphologies were different when copper salt was changed, the experimental at room temperature was observed. When thiourea were respectively added into the two kinds of cupric salt solutions containing the same amount of $CuSO_4{\cdot}5H_2O$ or $Cu(Ac)_2{\cdot}H_2O$ (1 mmol) under stirring, blue floccules occurred immediately in $CuSO_4{\cdot}5H_2O$ solution but no changes occurred in $Cu(Ac)_2{\cdot}H_2O$ solution. With the stirring continued, a white precipitate was formed. That was to say, the sulfate ions in the reaction system weakened the coordination of copper ions and –NH3 of the chitosan, so that the morphologies of obtained products were not changed. This showed the negative ions had a significant effect on the reaction process, which affected morphologies and structure of sample further.

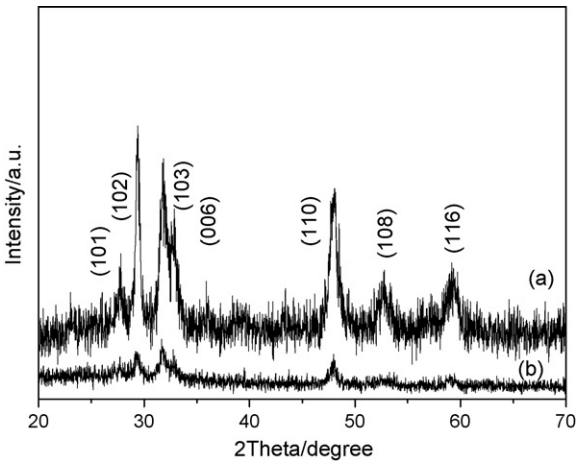

Fig. 6. XRD patterns of as-obtained CuS samples via different copper sources as reagent. (a) Copper sulfate and (b) copper acetate.

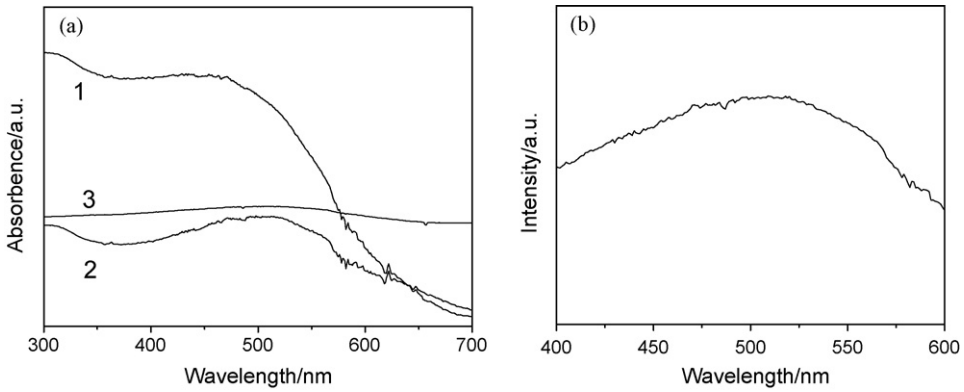

Fig. 7. UV–vis spectra of different CuS samples in (a): (1) $Cu(Ac)_2$ as reagent and reaction temperature at 100 °C; (2) $Cu(Ac)_2$ as reagent and reaction temperature at 140 °C; (3) $CuSO_4$ as reagent and reaction temperature at 140 °C. (b) The partly amplified curve 3.

A detailed discussion on XRD was made to verify further the change of structures of samples with the different resources of copper. The patterns were exhibited in Fig. 6. All diffraction peaks in two curves could be indexed to the hexagonal CuS (JCPDS 06-0464), which showed that the same hexagonal CuS samples were obtained when copper source was changed. But the lattice constants changed from $a = 3.804$ Å, $c = 16.378$ Å (copper acetate as copper source) to $a = 3.785$ Å and $c = 16.355$ Å (copper sulfate as copper source). All these results revealed that crystal phase of products did not affected by different copper sources but the degree of crystallization was different. The appearance of broadening of peak in the copper acetate reaction system showed that the size of CuS crystalline was smaller than the size of CuS prepared in the copper sulfate reaction system. That was to say that the combined action of acetate ions and chitosan prevented fine particles from aggregating and helped to form structure with porosity.

To investigate the relation of morphologies and properties, UV–vis absorption property of CuS samples with different morphologies were examined in Fig. 7. In the figure, curves 1 and 2 were UV–vis absorption spectra of CuS samples used copper acetate as source and curve 3 was UV–vis absorption spectrum of CuS samples used copper sulfate as source. The peak of curve 3 could hardly be observed in the amplified image, which implied CuS sample had a very weak absorption when copper sulfate was used as source. However, the broad absorption peaks were observed in curves 1 and 2, which revealed that obtained CuS samples used copper acetate as source had fine particles size. Maybe the quantum effect induced by smaller size of particles resulted in the broad and strong absorption. Moreover the absorption peak of three curves appeared at 429 nm, 498 nm, and 509 nm, respectively. In other words blue shift with different degrees occurred in curves 1 and 2 and the phenomenon of blue shift was more distinct when particle size decreased further. The different results of UV–vis were correspond to the SEM results and TEM results and indicated that the morphologies and structures of products affected their properties to a great degree.

The formation mechanism of CuS nanostructure with porosity was also discussed. Recently, biomolecule-assisted synthesis has been developed to prepare various novel nanomaterials because biomolecules have special structures and unique self-assembled functions which make them templates for the design and synthesis of complicated structures in the nanometer or submicrometer scale. As an available macromolecule, chitosan, as the deacetylated form of chitin and abundant naturally occurring polysaccharide, has been widely researched because of its linear polymer of acetylamino-D-glucose, the high contents of amino functional groups, excellent biodegradability, biocompatibility, antimicrobial activity and accelerated wound-healing properties [25–28]. In the reaction systems, the correlation of copper ions and NH_2^+ of chitosan formed bridging ligands, following with the attack of sulfur ions. The CuS sample with porosity was obtained after NH_2^+ of chitosan left. During this process, the presence of chitosan was crucial for the formation of porous structure because of its repulsion of NH_2^+ group and correlation effect with Cu^{2+}. When the temperature rose, the fine particles became more active which made the effective collision increased and deviation of chitosan easier. When clearance among particles decreased gradually with the rise of temperature, obtained CuS samples changed from porous structure to solid three-dimensional superstructure.

4. Conclusion

In a word, CuS nanospheres with porous structure were obtained via chitosan as template under hydrothermal condition. The BET surface area was measured to be 31.72 m^2/g and the single point adsorption total pore volume was measured to be 0.1367 cm^3/g. But changing copper salt, this kind of porous structure cannot be obtained. The UV–vis absorption of CuS samples with different morphologies was observed and the phenomenon of blue shift appeared. It implied that the morphologies and structure of samples affected their properties. The formation mechanism was also proposed based on the electron microscope images and parallel experiments.

Acknowledgements

The authors are grateful to the financial support of the National Natural Science Foundation of China (No. 50772074), the State Major Research Plan (973) of China (No. 2006CB932302), and the Nano-Foundation of Shanghai in China (No. 0852nm01200), and the Shanghai Key Laboratory of Molecular Catalysis and Innovative Materials (No. 2009KF04).

References

[1] C.B. Murray, D.J. Norris, M.G. Bawendi, J. Am. Chem. Soc. 115 (1993) 8706.
[2] X. Peng, L. Manna, W.D. Yang, J. Wickham, E. Scher, A. Kadavanich, A.P. Alivisatos, Nature 404 (2000) 59.
[3] L. Manna, E.C. Scher, A.P. Alivisatos, J. Am. Chem. Soc. 122 (2000) 12700.
[4] L. Li, J. Hu, W. Yang, A.P. Alivisatos, Nano Lett. 1 (2001) 34.
[5] N. Pinna, K. Weiss, J. Urban, M.P. Pileni, Adv. Mater. 13 (2001) 261.
[6] T. Sakamoto, H. Sunamura, H. Kawaura, Appl. Phys. Lett. 82 (2003) 3032.
[7] H. Boller, J. Alloys Compd. 480 (2009) 131.
[8] S. Mann, Angew. Chem. Int. Ed. 39 (2000) 3392.
[9] Y. Huang, X.F. Duan, C.M. Lieber, Small 1 (2005) 142.
[10] J. Yuan, K. Laubemds, Q. Zhang, S.L. Suib, J. Am. Chem. Soc. 125 (2003) 4966.
[11] Y.L. Hou, H.S. Kondoh, T.S.K. Ohta, Chem. Mater. 17 (2005) 3994.
[12] M.S. Toprak, B.J. McKenna, M. Mikhaylova, J.H. Waite, G.D. Stucky, Adv. Mater. 19 (2007) 1362.

[13] Y.S. Ding, X.F. Shen, S. Gomez, H. Luo, M. Aindow, S.L. Suib, Adv. Funct. Mater. 16 (2006) 549.
[14] Z.C. Wu, C. Pan, Z.Y. Yao, Q.R. Zhao, Y. Xie, Cryst. Growth Des. 6 (2006) 1717.
[15] L.H. Lu, A. Kobayashi, Y. Kikkawa, K. Tawa, Y. Ozaki, J. Phys. Chem. B 110 (2006) 23234.
[16] S.T. Lakshmikvmar, Sol. Energy Mater. Sol. Cells 32 (1994) 7.
[17] E. Ramli, T.B. Rauchfuss, C.L. Stern, J. Am. Chem. Soc. 112 (1990) 4043.
[18] E.J. Silvester, F. Grieser, B.A. Sexton, T.W. Healy, Langmuir 7 (1991) 2917.
[19] K. Wakamura, Phys. Rev. B 56 (1997) 11593.
[20] A. Etkus, A. Galdikas, A. Mironas, I. Simkiene, I. Ancutiene, V. Janickis, S. Kaciulis, G. Mattogno, G.M. Ingo, Thin Solid Films 391 (2001) 275.
[21] B.X. Li, Y. Xie, Y. Xue, J. Phys. Chem. C 111 (2007) 12181.
[22] X.P. Shen, H. Zhao, H.Q. Shu, H. Zhou, A.H. Yuan, J. Phys. Chem. Solids 70 (2009) 422.
[23] J. Liu, D.F. Xue, J. Cryst. Growth 311 (2009) 500.
[24] X.L. Yu, Y. Wang, H.L.W. Chan, C.B. Cao, Microporous Mesoporous Mater. 118 (2009) 423.
[25] S. Hirano, H. Seino, Y. Akiyama, in: C.G. Gebelein, C. Carraher (Eds.), Biotechnology and Bioactive Polymers, Plenum, New York, 1994, pp. 43–54.
[26] M.T. Qurashi, H.S. Blair, S.J. Allea, J. Appl. Polym. Sci. 46 (1992) 255.
[27] C.Y. Wel, S.M. Hudson, J.M. Mayer, J. Polym. Sci. Part A: Polym. Chem. 30 (1992) 2187.
[28] W.G. Malette, H.T. Euiglem, R.D. Gaines, Ann. Thorac. Surg. 35 (1983) 55.